Molecular Crystals and Liquid Crystals
Publication details, including instructions for authors and subscription information:
http://www.tandfonline.com/loi/gmcl20

Self-Diffusion of a Semiflexible Polypeptide in a Magnetically Aligned Liquid Crystalline Phase

G. J. Doucet [a] & P. S. Russo [a]
[a] Department of Chemistry and Macromolecular Studies Group, Louisiana State University, Baton Rouge, Louisiana, USA
Version of record first published: 22 Jan 2013.

To cite this article: G. J. Doucet & P. S. Russo (2013): Self-Diffusion of a Semiflexible Polypeptide in a Magnetically Aligned Liquid Crystalline Phase, Molecular Crystals and Liquid Crystals, 570:1, 67-75

To link to this article: http://dx.doi.org/10.1080/15421406.2012.711686

Mol. Cryst. Liq. Cryst., Vol. 570: pp. 67–75, 2013

ISSN: 1542-1406 print/1563-5287 online
DOI: 10.1080/15421406.2012.711686

Taylor & Francis
Taylor & Francis Group

Self-Diffusion of a Semiflexible Polypeptide in a Magnetically Aligned Liquid Crystalline Phase

G. J. DOUCET AND P. S. RUSSO*

Department of Chemistry and Macromolecular Studies Group, Louisiana State University, Baton Rouge, Louisiana, USA

The tracer self-diffusion coefficient of semiflexible poly(γ-benzyl-α,L-glutamate) with a length of ∼160 nm and a diameter of ∼1.6 nm is determined by fluorescence photobleaching recovery in the magnetically aligned liquid crystalline phase. The rate of diffusion in the direction of molecular alignment declines with concentration in the liquid crystalline phase, while the rate perpendicular to the direction of molecular alignment remains approximately constant. At concentrations just sufficient to sustain the liquid crystalline phase, the parallel diffusion exceeds the perpendicular diffusion by a factor of almost 5. This ratio declines to as little as 2 at higher concentrations. Comparisons are made with previous studies on other systems ranging from rigid virus particles to small mesogens.

Keywords Polymer liquid crystal; anisotropic diffusion; semiflexible polypeptides

Introduction

Molecules in a liquid crystalline (LC) phase remain nominally aligned, while retaining substantial mobility. The anisotropy of molecular motion has been explored in a number of contexts [1–14], partly as a matter of intrinsic interest, but also because on this property rest certain practical aspects of liquid crystals, such as heat dissipation, phase separation, and healing of defects. In the case of *polymer* liquid crystals, often made from semiflexible macromolecules [8,15,16], one may also include the role of diffusion in creating high-strength fibers by spinning from LC phases [17,18].

The semiflexible polypeptide poly(γ-benzyl-α,L-glutamate) (PBLG) played a historic role in the understanding of polymeric liquid crystals [15,16,19–21]. The director of PBLG liquid crystals can be aligned by surface effects [22] or by electric or magnetic fields [23–28], but normally PBLG assumes a cholesteric structure. In an earlier study of diffusion in PBLG liquid crystals [29,30], this twisted nematic feature and the special alignment of the screw axis normal to a cell wall was exploited to study the removal of topological constraints to mobility by slightly *raising* the concentration as the LC phase was entered. Some information about the anisotropy of diffusion was obtained in the process. In the present study, PBLG is aligned by magnetic field, and the optical tracer self-diffusion coefficient is directly measured parallel and perpendicular to the director. This results in a clearer interpretation of the anisotropy of motion.

*Address correspondence to P. S. Russo, Department of Chemistry and Macromolecular Studies Group, Louisiana State University, Baton Rouge, LA 70803, USA. E-mail: chruss@lsu.edu

It will prove convenient to reference our measurements to diffusion in dilute solution. The simplest theory for the diffusion of rod-like polymers, i.e. the theory of Kirkwood and Riseman [31], is sufficient for the present purposes. At zero concentration, the expectation for a rod of length L and diameter d is

$$D^{\mathrm{o}} = \frac{k_{\mathrm{B}} T \ln(L/d)}{3\pi\eta_{\mathrm{s}} L}, \tag{1}$$

where T is the temperature, η_{s} is the viscosity of the solvent, and k_{B} is Boltzmann's constant. The friction for perpendicular motion is twice that for parallel motion. It is conventional to express this difference inversely through diffusion coefficients [32–34]:

$$D^{\mathrm{o}}_{\perp} = \frac{1}{2} D^{\mathrm{o}}_{||}. \tag{2}$$

The average diffusion coefficient at infinite dilution is

$$D^{\mathrm{o}} = \frac{1}{3}(D^{\mathrm{o}}_{||} + 2D^{\mathrm{o}}_{\perp}) = \frac{2}{3} D^{\mathrm{o}}_{||} = \frac{4}{3} D^{\mathrm{o}}_{\perp}. \tag{3}$$

As the concentration rises, it is expected that perpendicular motion becomes difficult (the even-more-constrained rotational motion lies outside the scope of this work). Doi and Edwards (DE) [32,33] simply assumed that perpendicular motion ceases ($D_{\perp} = 0$), while parallel motion of a thin particle is unimpeded ($D_{||} = D^{\mathrm{o}}_{||}$). This results in the overall diffusion being reduced by half: $D = \frac{1}{2} D^{\mathrm{o}}$in the semidilute regime. Many advances have been made since the original DE work (see, for examples [35–37]), but the DE expectation of a 50% reduction in diffusion remains a convenient landmark. The diffusion of PBLG in the isotropic phase, most of which could be considered semidilute, declines much more than this; at the highest isotropic concentrations, the molecules retain only about 10% of their initial diffusivity [38]. Tobacco mosaic virus (TMV) comes closer to the DE expectation, despite its rather "fat" profile [39]. One might suppose that the extra rigidity of TMV accounts for better adherence to the DE expectation, but then it is difficult to explain why even short PBLG molecules shed all but ~10% of their initial diffusivity while still in the concentrated isotropic phase. Other rods and rod-like macromolecules have been considered too [40–45], but no complete and clear picture has emerged about diffusion, even in the isotropic phase.

This paper is devoted to exploring diffusion in the LC phase. Droplets of the LC phase, bathed in isotropic fluid, first appear at number density ν_{A}. Above a slightly higher number density, ν_{B}, the LC phase occupies all available space. For thin, extended, rigid rods, both ν_{A} and ν_{B} lie near the critical concentration identified by Onsager [46]:

$$\nu^* = \frac{16}{\pi d L^2}. \tag{4}$$

This corresponds to a volume fraction $\phi^* = 4d/L$. At low molecular weights, PBLG follows this prediction well [47], but for larger polymers molecular flexure defers the transition to a concentration of about two times greater, which fortuitously places the I-LC boundary closer to the expectation of Flory's lattice theory [48]. For example, the PBLG-232 sample studied has an experimentally determined $\phi_{\mathrm{A}} = 0.0932$, while the Onsager theory [46] predicts $\phi^* = 0.040$ based on the known molecular dimensions.

Table 1. Properties of PBLG

Sample	PBLG-232[a]
Nominal M/1000	232
M_n/1000	230
M_w/1000	276
PDI	1.2 (bimodal)
L (Å)	1590
L/d (at $d = 16$ Å)	99
ϕ^* (Onsager)	0.05
ϕ^* (Flory)	0.10
ϕ_A (Observed)	0.0932
$D^\circ/10^{-7}$ cm^2 s^{-1}	1.46
$D^\circ/10^{-7}$ cm^2 s^{-1} (Kirkwood–Riseman)	1.37
$D^A/10^{-7}$ cm^2 s^{-1}	0.15

[a][29].

Experimental

Materials and Characterization

PBLG-232 purchased from Sigma was labeled and characterized as previously described [29,30]. Its characteristics are shown in Table 1. Perhaps most notable are the molecular weight, 232,000 g/mol, and the good agreement of the measured, zero-concentration diffusion coefficient with the Kirkwood–Riseman expectation (Eq. (1)). Anhydrous pyridine was obtained from Fisher.

Sample Preparation

To prevent self-quenching of the fluorescence, measurements were made at a constant concentration of labeled material. To this end, a "pseudosolvent" containing labeled polymer was prepared and used to dissolve unlabeled polymer. The pseudosolvent was prepared by dissolving LPBLG in anhydrous pyridine at a weight fraction, w, of 0.01 (1%). To prevent water contamination, the pseudosolvent was stored over activated molecular sieves that had been rinsed five times with anhydrous pyridine to reduce dust. Concentrated solutions were made by dissolving unlabeled PBLG with the pseudosolvent. When computing the solute concentration, labeled and unlabeled PBLG are included. Measurements were conducted in rectangular capillaries with a path length of 200 μm (Vitrocom Inc.). The viscous samples were drawn into the capillaries by flame sealing on one end and inserting the cool, open end into the liquid crystal; as the warm end cools, the resulting vacuum suffices to draw the required volume ($\sim$5 μL) into the capillary. After low-speed centrifugation to place the sample near the end first heated (now cool), the other end of the capillary was sealed in flame to prevent moisture contamination. The LPBLG/PBLG/pyridine solution was diluted with additional pseudosolvent and a new weight fraction of LPBLG plus PBLG was calculated. Just two or three dilutions were made from one concentrated stock solution to limit the accumulation of error. After that a fresh stock solution was prepared from solid polymer and pseudosolvent. Conversions from weight fraction to volume fraction [30] were

computed using partial specific volumes, assumed constant, of 1.023 mL/g for pyridine and 0.791 mL/g for PBLG. The former value is the inverse of the density of pyridine[1] at 25°C; the latter is actually for PBLG in Dimethylformamide (DMF) [49], but surely close to the pyridine value. The loaded samples were equilibrated for four days.

Fluorescence Photobleaching Recovery Measurements

Fluorescence Photobleaching Recovery (FPR) measurements were conducted at 25.00 ± 0.01°C. The modulated detection method used is described in detail elsewhere [50,51]. Briefly, the image of a striped glass is created in the fluorescent sample by projecting a 488-nm laser beam into the solution. First, the fluorescence arising from the bright parts of the pattern is measured. Next, in the bright parts of the pattern, 5–10% of the dyes attached to the macromolecules are destroyed by an intense, brief flash of light at nearly the full output of the laser (up to 1 watt is available). The contrast of the resulting pattern is determined while illuminating the sample at low intensity (some 2000× lower than the bleaching pulse) using a modulated detector scheme similar to that developed by Lanni and Ware [52]. If all labeled molecules have the same diffusion coefficient D, the signal is an exponential decay with decay rate, $\Gamma = K^2 D$, where $K = 2\pi/l$ and l is the spatial period of the striped pattern in the sample.

Magnetic Alignment

The samples were aligned by placing the rectangular glass capillary tubes in a 500-MHz Nuclear Magnetic Resonance (NMR) spectrometer (11.7 Tesla magnetic field). Each sample was first inserted into a standard NMR tube for convenience. Even short exposures (30 min) to such a high field were sufficient to align the liquid crystals. FPR measurements were conducted as soon as practical after removal from the NMR (several minutes). Moderately longer waits had no effect on the results.

Results and Discussion

As shown in Fig. 1, the diffusion parallel to the magnetic field always exceeds that perpendicular to it. Comparison to the isotropic phase data (see Fig. 3 of [29]) shows that the perpendicular diffusion is a bit slower than the remaining diffusion in the isotropic state just prior to the I-LC transition, while the parallel motion significantly exceeds that value. From Eq. (3), the expected value of the parallel-to-the-rod component of diffusion at infinite dilution is $D^{\circ}_{||} = \frac{3}{2} D^{\circ}$. Consulting Table 1, $D^{\circ}_{||} = 2.19 \times 10^{-7}$ cm^2 s^{-1} or about 4.3 times faster than the parallel diffusion in the most dilute LC phase, where $D^{\mathrm{B}} = 5.04 \times 10^{-8}$ cm^2 s^{-1} (the superscript B refers to the lowest measured LC concentration, close to the conventionally defined B-point [46]). Alternately, one can write $D^{\mathrm{B}}_{||}/D^{\circ}_{||} = 0.23$. The parallel motion continues to decline in the LC phase. For the perpendicular-to-the-rod component, one may expect $D^{\circ}_{\perp} = \frac{3}{4} D^{\circ} = 1.095 \times 10^{-7}$ cm^2 s^{-1}. At any concentration in the aligned LC phase, the perpendicular component is essentially 10 times lower than this zero-concentration value; the average value was $D^{\mathrm{LC}}_{\perp} = 1.16 \pm 0.25 \times 10^{-8}$ cm^2 s^{-1}.

[1]Comprehensive information about pyridine (CAS Number 110-86-1) appears in The Beilstein Handbook (System Number 3051: vol 20, p. 181; 1st supplement, Vol. 20, p. 54; 2nd supplement, Vol. 20, p. 96, 4th supplement, Vol. 20, p. 2205).

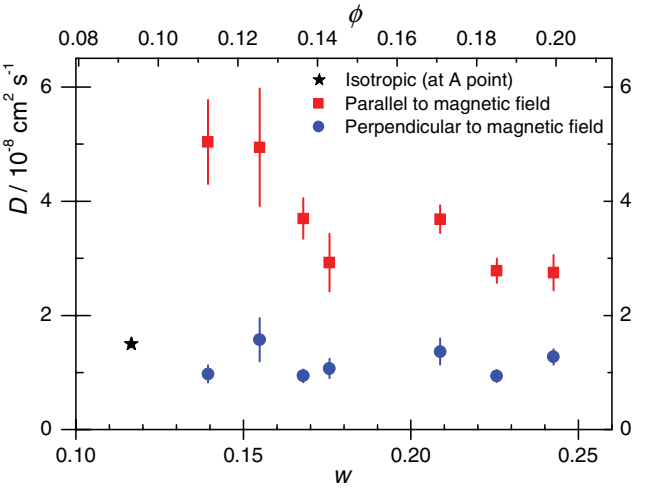

Figure 1. Diffusion of LPBLG-232 at a fixed weight fraction (∼1%) as a function of summed weight fraction of LPBLG-232 and PBLG-232.

Comparison with the previous results [29,30] on z-aligned cholesteric LCs (z denotes the direction perpendicular to the capillary cell wall) is complicated by the radially averaged alignment of the rods with respect to the FPR instrument's striped pattern and by the assumptions required previously (see Table 2 of [30]).

Several authors have related diffusion anisotropy to the order parameter S [6, 53]. For thin, rigid rods, we may write [53]:

$$S = \frac{D_{||} - D_{\perp}}{D_{||} + 2D_{\perp}}. \tag{5}$$

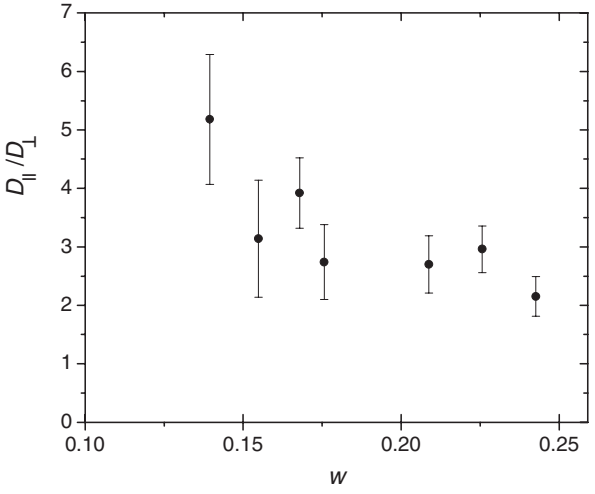

Figure 2. Quotient of parallel and perpendicular diffusion for LPBLG-232 at a fixed weight fraction (∼1%) as a function of summed weight fraction of LPBLG-232 and PBLG-232.

It may be shown (see [9,30]) that

$$\frac{D_{||}^{LC}}{D_{\perp}^{LC}} = \frac{2S+1}{1-S}. \tag{6}$$

For PBLG LCs, S ranges from about 0.53 to 0.75 [28,54,55], which corresponds to $D_{||}^{LC}/D_{\perp}^{LC}$ values of 4.4 to 10 respectively. Our result (see Fig. 2) that $D_{||}^{LC}/D_{\perp}^{LC} = 5.2$ at a concentration just high enough to sustain the LC phase is in the specified range, but at the highest concentrations $D_{||}^{LC}/D_{\perp}^{LC}$ decreased to 2.2. The downward trend in $D_{||}$ but not $D_{\perp}$ is intriguing. At the length measured here, PBLG in dilute solution behaves as a semiflexible filament. There seems to be little information on whether the polymer straightens as it enters the LC phase, but its intrinsic tendency to flex would not be expected to disappear completely. Such bending and the finite diameter ensure that PBLG cannot behave as a thin needle, but it is not easy to separate these two effects. Instability of the helix at the ends of the chain is another potential factor. For whatever reason, the lengthwise motion of the filaments experiences increasing hindrance in the nematic phase, while the sideways motion does not.

Additional insight can be gained by considering related studies, which are relatively few in number. Dvinskikh and colleagues [56,57] used pulsed field gradient NMR (PFGNMR) to determine the self-diffusion anisotropy of 5CB(4-n-pentyl-4′-cyanobiphenyl). They obtained $D_{||}^{LC}/D_{\perp}^{LC} = 2.7$ at low temperatures. As discussed in [56], this exceeds previous determinations by a variety of methods. The work by Dvinskikh et al. [56,57] is a convenient point of reference, but the axial ratio of the thermotropic 5CB mesogen is much lower than that of the PBLG macromolecules of the present work, which form lyotropic liquid crystals.

Barbara and coworkers [2,9] developed a two-beam cross-correlation fluorescence method to study the anisotropic diffusion of MEH-PPV (poly[2-methoxy-5-(2-ethylhexyloxy)-1,4-phenylenevinylene]) dissolved in 5CB and a related mesogenic solvent, 8CB (4-n-octyl-4′-cyanobiphenyl). MEH-PPV is an extended polymer, and is aligned well in LC solvents. Even so, the authors observed only a small diffusion anisotropy, $D_{||}^{LC}/D_{\perp}^{LC} = 1.9 \pm 0.3$, for solvents in the nematic phase. As the authors pointed out, this is lower than expected based on the order parameter of the mesogenic solvent and much lower than expected based on the effective axial ratio and stiffness of MEH-PPV.

Lettinga et al. [1] used fluorescence microscopy to follow the trajectories of labeled fd virus through isotropic and nematic solutions of unlabeled fd virus. At the isotropic-to-nematic transition, $D_{||}$ rose suddenly above the isotropic diffusion value, while $D_{\perp}$ fell. As the virus concentration increased, there was, overall, a decrease in both diffusion coefficients. The data suggest a plateau in $D_{||}$ just above the I-N transition, but it is difficult to distinguish its extent given the experimental uncertainty. The ratio $D_{||}^{LC}/D_{\perp}^{LC}$ climbed from $\approx$7.5 just above the I-N transition to >10 (and even higher as concentration rose toward the value required to sustain a smectic phase). These results on fd virus have similarities and differences from the present experiments on PBLG. In both cases, $D_{||}$ increased markedly above the isotropic value as the LC phase was entered; however, $D_{\perp}$ decreased for fd, while little change was observed for PBLG. Both diffusers are semiflexible filaments, but fd behaves more like a stiff rod than PBLG does at the length chosen for study. (The contour length of fd is less than half its persistence length, while the PBLG sample studied here has a contour length comparable to its persistence length, the value of which remains in dispute; see, for example, Temyanko et al. [58]). Both fd and PBLG are more flexible than the colloidal boehmite rods studied by van Bruggen et al. using FPR [44]. In that system,

both $D_{||}$ and $D_{\perp}$ were less in the nematic phase than in the coexistent isotropic phase, and $D_{||}^{LC}/D_{\perp}^{LC} \approx 2$.

Yin et al. [59] used PFGNMR to measure poly(γ-stearyl-L-glutamate), PSLG, that had been prepared from PBLG with molecular weight of 30,000 by ester exchange with octadecyl (stearyl) alcohol. Diffusion was greatly reduced in the LC phase, but this observation is colored by the finding that even in the isotropic phase the diffusion coefficients exceeded expectations based on Eq. (1). The expected molecular weight of the PSLG studied was 52,000 (30,000 × 382/219 where 382 and 219 are the molecular weights of the SLG and BLG monomers respectively) corresponding to a length of 20 nm. Inserting the diameter of PSLG (3.6 nm [58]) and the viscosity of chloroform (0.569 cP) into Eq. (1) yields $D \approx 7 \times 10^{-7}$ cm^2 s^{-1}. The measured diffusion coefficient in the isotropic phase was almost four times larger. The reason for this is not understood, but problems with using PFGNMR to measure diffusion coefficients of rod-like polymers have been noted previously [60].

An intriguing study by Ilg [10] introduced a kinetic model of diffusion, which unifies liquid crystals and ferromagnetic fluids. This author predicts a significant increase in parallel diffusion accompanied by a substantial decrease in perpendicular diffusion as the order parameter increases. For order parameters nearing 1, the results of Fig. 4 of [10] are consistent with $D_{||}^{LC}/D_{\perp}^{LC} \sim 3.5$.

Conclusion

In a magnetically aligned LC phase of the semiflexible helical polymer, PBLG, the diffusion coefficient measured parallel to the director exceeded that measured perpendicular to it by a factor of 2–5, depending on concentration. The variation can be attributed to reductions in the parallel component of diffusion, while motion perpendicular to the rod axis was relatively unaffected. The most obvious explanation seems to be the semiflexibility of the chain, which would raise the average cross section for motions nominally parallel to the axis while not affecting lateral friction. Chain flexure is not the only possibility, though. The stiff character of polypeptides is a consequence of the helical conformational state. The effect of partial helix unwinding, even on a transient basis, is not known. Experiments to tease apart these two effects may involve co-solvents to prod the polypeptide toward its helix-coil transition at readily achieved temperatures, selective deuterium labeling to permit NMR investigation of the conformation and better understanding of the flexure of the molecule as it exists in the LC phase. Perhaps more than anything else, similar experiments on other helical and non-helical semiflexible polymers are required.

Acknowledgment

This material is based upon work supported by the National Science Foundation under Grants 0606117 and 1005707 (DMR).

References

[1] Lettinga, M. P., Barry, E., & Dogic, Z. (2005). *Europhys. Letts.*, *71*, 692–698.
[2] Link, S., Chang, W. S., Yethiraj, A., & Barbara, P. F. (2006). *J. Phys. Chem. B*, *110*, 19799–19803.
[3] Yun, C. K., & Fredrickson, A. G. (1970). *Mol. Cryst. Liq. Cryst.*, *12*, 73–91.
[4] Otnes, K., Pynn, R., Janik, J. A., & Janik, J. M. (1972). *Phys. Letts.*, *38A*, 335–336.
[5] Daoud, M., Gharbia, M., & Gharbi, A. (1994). *J. Phys. II France*, *4*, 989–1000.
[6] Chu, K. S., & Moroi, D. S. (1975). *J. de Physique Colloque C1*, *36*, 99–101.

[7] Blinc, R., Hogenboom, D. L., O'Reilly, D. E., & Peterson, E. M. (1969). *Phys. Rev. Lett.*, *23*, 969–972.
[8] Bellomo, E. G., Davidson, P., Imperor-Clerc, M., & Deming, T. J. (2004). *J. Am. Chem. Soc.*, *126*, 9101–9105.
[9] Barbara, P. F., Chang, W. S., Link, S., Scholes, G. D., & Yethiraj, A. (2007). *Ann. Rev. Phys. Chem.*, *58*, 565–584.
[10] Ilg, P. (2005). *Phys. Rev. E*, *71*, 051407-1–051407-9.
[11] Munk, T., Hofling, F., Frey, E., & Franosch, T. (2009). *EPL*, *85*.
[12] Vasanthi, R., Bhattacharyya, S., & Bagchi, B. (2002). *J. Chem. Phys.*, *116*, 1092–1096.
[13] Han, Y. L., Alsayed, A., Nobili, M., & Yodh, A. G. (2009). *Phys. Rev. E*, *80*, 80.011403.
[14] Allen, M. P. (1990). *Phys. Rev. Lett.*, *65*(23), 2881–2884.
[15] Miller, W. G. (1978). *Annu. Rev. Phys. Chem.*, *29*, 519–535.
[16] Uematsu, I., & Uematsu, Y. (1984). *Adv. Polym. Sci.*, *59*, 37–73.
[17] Kwolek, S. L., Morgan, P. W., & Schaefgen, J. R. (1987). In Encyclopedia of Polymer Science, 2nd edition, H.F. Mark, N.M. Bikales, C.G. Overberger, G. Menges and J. I. Kroschwitz, eds., Vol. 9, Wiley Interscience, New York, New York, 1987, p. 1–61.
[18] Magat, E. E. (1980). *Philos. Trans. Roy Soc A*, *294*, 463–472.
[19] Robinson, C. (1956). *Trans. Faraday Soc.*, *52*, 571–592.
[20] Robinson, C., Ward, J. C., & Beevers, R. B. (1958). *Disc. Far. Soc.*, *25*, 29–42.
[21] Robinson, C. (1966). *Mol. Cryst.*, *1*, 467–494.
[22] Taratuta, V. G., Srajer, G. M., & Meyer, R. B. (1985). *Mol. Cryst. Liq. Cryst.*, *116*, 245–252.
[23] Filas, R. W., Hajdo, L. E., & Eringen, A. C. (1974). *J. Chem. Phys.*, *61*, 3037–3038.
[24] Orwoll, R. D., & Vold, R. L. (1971). *J. Am. Chem. Soc.*, *93*, 5335–5338.
[25] Toyoshima, Y., Minami, N., & Sukigra, M. (1976). *Mol. Cryst. Liq. Cryst.*, *35*, 325–335.
[26] Tohyama, K., Miyata, N., & Honda, M. (1978). *J. Chem. Phys.*, *68*, 5490–5493.
[27] Gresser, J. D., Trantolo, D. J., Wise, D. L., & Wnek, G. E. US Patent *Nos.* 5512218, 3241994.
[28] Wagner, N. J., & Walker, L. M. (1994). *Macromolecules*, *27*, 5979–5986.
[29] Russo, P. S., Baylis, M., Bu, Z., Stryjewski, W., Doucet, G., Temyanko, E., & Tipton, D. (1999). *J. Chem. Phys.*, *111*, 1746–1752.
[30] Doucet, G. J., Qiu, J., & Russo, P. S. (2010). *J. Phys. Chem. B*, *114*, 4777–4782.
[31] Riseman, J., & Kirkwood, J. G. (1950). *J. Chem. Phys.*, *18*, 512–516.
[32] Doi, M., & Edwards, S. F. (1978). *J. Chem. Soc. Far. Trans.* Pt. 2, *74*, 560–570.
[33] Doi, M., & Edwards, S. F. (1978). *J. Chem. Soc. Far. Trans.* Pt. 2, *74*, 918–932.
[34] Tracy, M. A., & Pecora, R. (1992). *Annu. Rev. Phys. Chem.*, *43*, 525–557.
[35] Otto, M., Aspelmeier, T., & Zippelius, A. (2006). *J. Chem. Phys.*, *124*.
[36] Szamel, G., & Schweizer, K. S. (1994). *J. Chem. Phys.*, *100*, 3127–3141.
[37] Teraoka, I., & Hayakawa, R. J. (1988). *J. Chem. Phys.*, *89*, 6989–6995.
[38] Bu, Z., Russo, P. S., Tipton, D. L., & Negulescu, I. I. (1994). *Macromolecules*, *27*, 6871–6882.
[39] Cush, R. C., & Russo, P. S. (2002). *Macromolecules*, *35*, 8659–8662.
[40] Tinland, B., Maret, G., & Rinaudo, M. (1990). *Macromolecules*, *23*, 596–602.
[41] Seils, J., & Pecora, R. (1994). *Macromolecules*, *28*, 661–673.
[42] Wang, L., Garner, M. M., & Yu, H. (1991). *Macromolecules*, *24*(9), 2368–2376.
[43] Scalettar, B. A., Hearst, J. E., & Klein, M. P. (1989). *Macromolecules*, *22*, 4550.
[44] van Bruggen, M., Lekkerkerker, H. N. W., Maret, G., & Dhont, J. K. G. (1998). *Phys. Rev. E*, *58*, 7668–7677.
[45] van Bruggen, M., Lekkerkerker, H. N. W., & Dhont, J. K. G. (1997). *Phys. Rev. E*, *56*, 4394–4403.
[46] Onsager, L. (1949). *Ann. N.Y. Acad. Sci.*, *51*, 627–659.
[47] Kubo, K., & Ogino, K. (1979). *Mol. Cryst. Liq. Cryst.*, *53*, 207–227.
[48] Flory, P. J. (1984). *Adv. Polym. Sci.*, *59*, 2–36.
[49] Mitchell, J. C., Woodward, A. E., & Doty, P. (1957). *J. Am. Chem. Soc.*, *79*, 3955–3960.
[50] Russo, P. S., Qiu, J., Edwin, N., Choi, Y.-W., Doucet, G., & Sohn, D., (2008) In Soft Matter Characterization, R. Borsali and R. Pecora, eds., Kluwer, New York, New York, pages 605–636, Ch. 10.

[51] Bu, Z., & Russo, P. S. (1994). *Macromolecules*, *27*, 1187–1194.
[52] Lanni, F., & Ware, B. R. (1982). *Rev. Sci. Instrum.*, *53*(6), 905–908.
[53] Hess, S., Frenkel, D., & Allen, M. P. (1991). *Mol. Phys.*, *74*, 765–774.
[54] Walker, L. M., & Wagner, N. J. (1996). *Macromolecules*, *29*, 2298–2301.
[55] Murthy, N. S., Knox, J. R., & Samulski, E. T. (1976). *J. Chem. Phys.*, *65*, 4835–4839.
[56] Dvinskikh, S. V., & Furo, I. (2001). *J. Chem. Phys.*, *115*, 1946–1950.
[57] Furo, I., & Dvinskikh, S. V. (2002). *Mag. Res. Chem.*, *40*, S3–S14.
[58] Temyanko, E., Russo, P. S., & Ricks, H. (2001). *Macromolecules*, *34*, 582–586.
[59] Yin, Y. G., Zhao, C. H., Sasaki, A., Kimura, H., Kuroki, S., & Ando, I. (2002). *Macromolecules*, *35*, 5910–5915.
[60] Baldwin, A. J., Anthony-Cahill, S. J., Knowles, T. P. J., Lippens, G., Christodoulou, J., Barker, P. D., & Dobson, C. M. (2008). *Angewandte Chemie Int. Ed.*, *47*, 3385–3387.